Journal of Sound and Vibration 329 (2010) 3008–3019

Contents lists available at ScienceDirect

Journal of Sound and Vibration

journal homepage: www.elsevier.com/locate/jsvi

A state space force identification method based on Markov parameters precise computation and regularization technique

Y.M. Mao *, X.L. Guo, Yan Zhao

State Key Laboratory of Structure Analysis for Industry Equipment, Dalian University of Technology, Dalian, China

ARTICLE INFO

Article history:
Received 2 June 2009
Received in revised form
28 January 2010
Accepted 10 February 2010
Handling Editor: L.G. Tham
Available online 4 March 2010

ABSTRACT

A time domain force identification approach for linear system is proposed. This approach can found a highly precise force identification model within the scope of general computer precision while it does not cost much computing time. Although the force identification model is accurate, the force identification process, like other inverse methods, is still ill-posed due to the inversion process and the white noise in measured structural responses. The singular value decomposition is used to reveal the intrinsically matter of the ill-posedness of force identification problem and a regularization technique is utilized to deal with this issue. Finally, the proposed method with the aid of regularization technique is successfully applied to identify the input forces in two numerical simulations.

1. Introduction

Accurately knowledge of the dynamic forces acting on a physical structure through its designated life can be very important component in the design of mechanical systems, from spacecraft and processing plants to electronic circuits. Regardless of actual application or the underlying physics, the expected force will play a key role in the determination of system properties or parameters. Unfortunately, in many practical situations, it is difficult, if not impossible, to perform direct measurements or calculations of the external forces acting on vibrating structures. Especially, in some cases, if force gauges are inserted into force transfer path to measure those dynamic forces directly, these force gauges may either alter the system properties or intrude on the load path. Instead, vibration responses can often be conveniently measured. In such cases indirect estimating these dynamic forces by the measured structural responses in some sort of inverse model is sometimes necessary, which means that unknown force is established as the solution to an inverse problem of force reconstruction, based on the measured system responses, i.e. the process is considered as estimating of unknown dynamic force acting on a mechanical system from measured responses.

In recent years various methods for solving the inverse problem associated with indirect force measurement have been proposed, see, e.g. Steven [1], Hirotsugu et al. [2], Dobson et al. [3] and Nordstron et al. [4] for an overview and Refs. [5–9] for more recent improvements to the force identification methods. Liu et al. [10] imposed a system identification technique to study the force identification on a cantilever plate in state space, where the forces were estimated from the measured systematic responses by an inverse algorithm, and the least-squares method with a recursive estimator is employed to update the estimation in the sense of real-time computation. Adam et al. [11] used the state space formulation to found the force identification model in time domain, in order to estimate six docking forces and moments between the Space Shuttle

* Corresponding author.
E-mail address: vibration_mao@yahoo.com.cn (Y.M. Mao).

0022-460X/$ - see front matter Crown Copyright © 2010 Published by Elsevier Ltd. All rights reserved.
doi:10.1016/j.jsv.2010.02.012

and the Russian MIR Station during a numerical simulation of a docking event. Nordberg and Gustafsson [12] presented an explicit block inversion algorithm to invert the associated upper block triangular Toeplitz matrix for reconstructing input forces. All these methods mentioned above have obtained excellent force identification results and they mainly focused on the effect of noise in the measured structural responses on force identification results, while seldom concerned the round error in the sense of computation. However, in force identification process, the round error in force identification model usually reduces the accuracy of force identification results and even leads to meaningless results. Hence, the establishment of precise force identification model is important to force estimation results. This paper mainly concerns the foundation of precision force identification model in the sense of computation and one part and parcel of this paper is to establish a precise force identification model based on an idea of precise time-step integration method for Markov parameters (PTIM-MP), which was originally presented to compute the forward problem of structural dynamics [13]. In this work, we extend this approach to the inverse problem of force identification and found a highly accurate force identification model within the scope of general computer precision.

Like other force identification methods, although the force identification model founded by PTIM-MP is precise, the force identification problem is still ill-posed due to the inversion process and the white noise in the measured responses. And the white noise may destroy the identified inputs if it is not treated properly. Jacquelin et al. [14] utilized the regularization methods to solve the ill-posed force identification problem, where they discussed different regularization methods to the force identification problem. Liu et al. [15] proposed a regularization algorithm to solve the inverse of an ill-conditioned frequency response function matrix at near the frequencies of structural resonances, where the truncated singular value decomposition filter and Tikhonov filter were used in conjunction with the conventional least schemes and the optimum regularization parameters of these filters were selected by the Morozov's discrepancy principle. Finally, a total least-square scheme was also used to address the errors associated with the frequency response function matrix. In force identification problem, the difficulties arise due to sensitivity to measurement uncertainties, and the small measurement error could introduce a high noise level in the identification results. Hence, another aim of this paper is to cope with the ill-posed problem in force identification process and the inherent ill-posedness of force identification problem is disclosed with a useful numerical tool, the singular value decomposition. Finally, a Tikhonov regularization technique is used to solve this ill-posed problem of force reconstruction, and the optimum regularization parameter is determined by the generalized cross-validation (GCV) criterion [16].

In order to reconstruct the input force, this paper presents an algorithm based on PTIM-MP method with the aid of regularization technique. The PTIM-MP method can found a highly precision force identification model in the scope of general computer precision, while costs less computing time. The regularization technique is used to improve the stability in the solution of precise force identification model. This paper is organized as following: In Section 2 the force reconstruction algorithm based on an idea of PTIM-MP is developed briefly. The intrinsically ill-posedness of force identification problem is disclosed in Section 3, and the regularization solution of this ill-posed problem is also depicted in this section. In Section 4, the force reconstruction algorithm based on PTIM-MP is illustrated by two numerical tests. Finally, some concluding remarks are summarized in Section 5.

2. Force identification of PTIM-MP in state space

2.1. Moving average model (MAM) for force identification

Consider the following generally time invariant linear system governing equation in state space,

$$\dot{\mathbf{v}}(t)=\mathbf{H}\mathbf{v}(t)+\mathbf{f}(t) \tag{1}$$

The Eq. (1) is expressed as a Hamiltonian system, where $\mathbf{v}(t)$ the response vector in state space, $\mathbf{H}$ the system matrix in state space, $\mathbf{f}(t)$ the force vector in state space. The detailed derivation of Eq. (1) from a second order differential equation of structural system excited by a force is shown in Appendix A. Supposing that the eternal force in time step of integration is constant, the Eq. (1) can be discretized as Eq. (2) with the exponential matrix superposition algorithm.

$$\mathbf{v}(k+1)=\mathbf{T}\mathbf{v}(k)+(\mathbf{T}-\mathbf{I})\mathbf{H}^{-1}\mathbf{f}(k),\quad (k=0,1,2,\ldots,N_t) \tag{2}$$

where $\mathbf{T}=\exp(\mathbf{A}\Delta t)$ is the exponential matrix, whose computation will be further discussed in Section 2.2. Δt is the time step of integration, and N_t is the number of sampling points in time domain. $\mathbf{I}$ is the identity matrix. The detailed derivation of Eq. (2) is displayed in Appendix A. The quantities $\mathbf{y}_m(t)$ are assumed to be the measured responses in this work, and the observation quantity has the following relationships,

$$\mathbf{y}_m(k+1)=\mathbf{D}_m\mathbf{v}(k+1)=\mathbf{H}_k^0\mathbf{v}(t_0)+\sum_{i=0}^{k}\mathbf{H}_i\mathbf{f}(k-i) \tag{3}$$

$$\mathbf{y}(k+1)=\mathbf{y}_m(k+1)-\mathbf{H}_k^0\mathbf{v}(t_0)=\sum_{i=0}^{k}\mathbf{H}_i\mathbf{f}(k-i) \tag{4}$$

$$\mathbf{H}_i^0=\mathbf{D}_m\mathbf{T}^i\quad \mathbf{H}_i=\mathbf{D}_m\mathbf{T}^i(\mathbf{T}-\mathbf{I})\mathbf{H}^{-1} \tag{5}$$

where $\mathbf{D}_m$ the extract matrix, has the element of zeros or ones, matching the degree-of freedom (DOF) corresponding to the measured response components. For simplicity in formulation, the Eq. (3) can be written as Eq. (4), $\Delta\mathbf{y}(k+1)$ denote the differences between the measured quantities $\mathbf{y}_m(k+1)$ and the quantities $\mathbf{H}_k^0\mathbf{v}(t_0)$, $\mathbf{v}(t_0)$ is the initial condition of structural system, if the structural system is at rest before the external is applied, the quantities $\Delta\mathbf{y}(k+1)$ are equivalent to $\mathbf{y}_m(k+1)$. The Eq. (4) represents a moving average model of a discrete system, where the weighting matrix $\mathbf{H}_i$ are called Markov parameters and $\mathbf{H}_i^0$ is a parameter matrix related to initial condition $\mathbf{v}(t_0)$. Eq. (4) can be further formulated as Toeplitz matrix forms

$$\begin{Bmatrix} \Delta\mathbf{y}(N_t) \\ \Delta\mathbf{y}(N_t-1) \\ \vdots \\ \Delta\mathbf{y}(1) \end{Bmatrix} = \begin{Bmatrix} \mathbf{y}_m(N_t) \\ \mathbf{y}_m(N_t-1) \\ \vdots \\ \mathbf{y}_m(1) \end{Bmatrix} - \begin{bmatrix} \mathbf{H}_{N_t}^0 \\ \mathbf{H}_{N_t-1}^0 \\ \vdots \\ \mathbf{H}_1^0 \end{bmatrix} \mathbf{v}(t_0) = \begin{bmatrix} \mathbf{H}_0 & \mathbf{H}_1 & \cdots & \mathbf{H}_{N_t-1} \\ \vdots & \mathbf{H}_0 & & \mathbf{H}_{N_t-2} \\ \vdots & \vdots & \ddots & \vdots \\ 0 & 0 & \cdots & \mathbf{H}_0 \end{bmatrix} \begin{Bmatrix} \mathbf{f}(N_t-1) \\ \mathbf{f}(N_t-2) \\ \vdots \\ \mathbf{f}(0) \end{Bmatrix} \tag{6}$$

Then, it is easily to recast as follows

$$\mathbf{y} = \overline{\mathbf{H}}\mathbf{f} \tag{7}$$

The Eq. (7) is the force identification model to reconstruct the time history of input force from the measured responses.

2.2. An algorithm based on precise time-step integration method for Markov parameter $\mathbf{H}_i$

The Markov parameter matrix $\mathbf{H}_i$ in $\overline{\mathbf{H}}$ determines the accuracy of MAM for force identification, therefore precise computation of exponential matrix $\mathbf{T}$ plays a key role. The recently proposed precise time-step integration scheme [13] for exponential matrix $\mathbf{T}$ is applied due to its stability and high precision to any desired degree, if necessary. Utilizing the precise time-step integration method, the time interval Δt can be further divided into $m = 2^N$ subsections, i.e. $\tau = \Delta t/2^N$. N can be any positive integer depending on the desired accuracy and equals to 20 in this paper. τcan be extremely small since$\Delta t$is not already large. Consequently, in the time interval Δt the matrix $\mathbf{T}$ can be computed with a truncated Taylor expansion as following.

$$\begin{cases} \mathbf{T} = \exp(\mathbf{A}\tau)^m = (\mathbf{I}+\mathbf{T}_{a,0})^m \\ \mathbf{T}_{a,0} \approx \mathbf{A}\tau + (\mathbf{A}\tau)^2/2! + (\mathbf{A}\tau)^3/3! + (\mathbf{A}\tau)^4/4! \\ \mathbf{T}_{a,i} = 2 \times \mathbf{T}_{a,i\text{-}1} + \mathbf{T}_{a,i-1} \times \mathbf{T}_{a,i-1} \end{cases} \tag{8}$$

and

$$(\mathbf{I}+\mathbf{T}_{a,0})^m = (\mathbf{I}+\mathbf{T}_{a,1})^{m/2} = (\mathbf{I}+\mathbf{T}_{a,2})^{m/4} = \cdots = (\mathbf{I}+\mathbf{T}_{a,N}) = \mathbf{T} \tag{9}$$

In the computation of Eq. (8) only the exponential series expansion is approximate. $\mathbf{T}_{a,0}$ omitts higher order items with an error in order of $10^{-30}O(\Delta t^5)$, which is already smaller than a general computer accuracy because of rounding error. In order to avoid the rounding error due to the computer precision, the third formulation in Eq. (8) is first computed, until the $\mathbf{T}_{a,N}$ is obtained, and then the Eq. (9) is used to compute the exponential matrix $\mathbf{T}$. The precise computation for exponential matrix $\mathbf{T}$ can be considered as an exact solution within the scope of general computer precision, i.e. the Markov parameter matrix $\mathbf{H}_i$ in matrix $\overline{\mathbf{H}}$ is highly accurate. It should be noted that it does not cost much computing time, and the computation process includes only 20 steps addition algorithm (in case N=20). Thus, the input force can be computed using highly precise MAM force identification model. Although the force identification model is highly precise, the force identification problem is still ill-posed due to the white noise in measured responses. Then we will deal with the solution of this ill-posed problem.

3. Regularized solution to the inverse problem of force identification

3.1. The ordinary least square solution and analysis of the ill-posedness for force identification problem

The force identification problem in Eq. (7) constitutes computation of the input sequence vector $\mathbf{f}$ from known measured responses $\mathbf{y}$. In general, solving the inverse problem in the least square sense corresponds in the algebraic problem that minimizes the norm of the residual as

$$\min\|\overline{\mathbf{H}}\mathbf{f}-\mathbf{y}\|_2^2 \tag{10}$$

with the straight forward solution

$$\mathbf{f}_{LS} = \overline{\mathbf{H}}^+\mathbf{y} \tag{11}$$

where $\mathbf{f}_{LS}$ denotes the ordinary least squares solution of Eq. (10). In general, it follows that the existence of a unique solution requires that the entire block matrix $\overline{\mathbf{H}}$ is of full column rank. Therefore, the number of sensors to measure the responses should be equal or larger than that of input forces to be identified. $\overline{\mathbf{H}}^+ = \left[\overline{\mathbf{H}}^{\mathrm{T}}\overline{\mathbf{H}}\right]^{-1}\overline{\mathbf{H}}^{\mathrm{T}}$ is the Moore–Penrose

pseudo inverse of $\overline{\mathbf{H}}$ and $\overline{\mathbf{H}}^{\mathrm{T}}$ is the transpose of $\overline{\mathbf{H}}$. For a case where the input numbers is equal to the measurement points, $\overline{\mathbf{H}}$ will be a square matrix and $\overline{\mathbf{H}}^{+}$ becomes the regular matrix inverse $\overline{\mathbf{H}}^{-1}$. Eq. (7) is a well-known ill-posed problem and the ordinary least square solution is always worthless in many situations of force identification [2–4]. The ill-posedness of the Eq. (7) is also related to the character of the Toeplitz matrix besides the white noise in measured responses. Hansen briefly mentioned Toeplitz matrix regularization algorithms in the monograph [17], and then he presented modern computational methods for treating the deconvolution and regularization problems along with the Toeplitz matrix in Ref. [18], where a singular valued decomposition as a useful numerical tool was used to reveal the character of the Toeplitz matrix. In this paper the singular valued decomposition is also used to disclose the ill-posedness of force identification problem, for readability, the singular valued decomposition will be introduced briefly, and then used to disclose the essence of the ill-posedness of the force identification problem.

For the sake of simplicity, let $\overline{\mathbf{H}} \in \mathbb{R}^{m\times n}$ be a rectangular matrix with $m \geq n$. Then the SVD of $\overline{\mathbf{H}}$ is as the following form

$$\overline{\mathbf{H}} = \mathbf{U}\Sigma\mathbf{V}^{\mathrm{T}} = \sum_{i=1}^{n} u_i \sigma_i v_i^{\mathrm{T}} \tag{12}$$

where $\mathbf{U} = (u_1 \cdots u_m)$ and $\mathbf{V} = (v_1 \cdots v_n)$ are the matrices with orthogonal columns, $\mathbf{U}^{\mathrm{T}}\mathbf{U} = \mathbf{V}^{\mathrm{T}}\mathbf{V} = \mathbf{I}$, and $\Sigma = diag(\sigma_1 \cdots \sigma_n)$ has non-negative diagonal elements appearing in non-increasing order such that $\sigma_1 \geq \cdots \geq \sigma_n \geq 0$. The elements σ_i are the singular values of $\overline{\mathbf{H}}$, while the vectors of u_i and v_i are the left and right singular vectors of $\overline{\mathbf{H}}$, respectively. Two characteristic features of the discrete ill-posed problem for force identification are usually found with the matrix theory [19]. One case is that the singular values σ_i decay gradually to zero with no particular gap in the spectrum and an increase of the dimensions of $\overline{\mathbf{H}}$ will increase the number of the small singular values. The other is that the left and right singular vectors of u_i and v_i tend to have more sign changes in their elements as the index $i$increases, i.e., as singular values σ_i decay. According to the singular value decomposition theory [19], the singular vectors have the following relations

$$\mathbf{U}^{\mathrm{T}}\mathbf{U} = \mathbf{V}^{\mathrm{T}}\mathbf{V} = \mathbf{I} \tag{13}$$

$$\overline{\mathbf{H}}\overline{\mathbf{H}}^{\mathrm{T}} = \mathbf{U}\Sigma^2\mathbf{U}^{\mathrm{T}} \tag{14}$$

$$\overline{\mathbf{H}}^{\mathrm{T}}\overline{\mathbf{H}} = \mathbf{V}\Sigma^2\mathbf{V}^{\mathrm{T}} \tag{15}$$

Consider the solution of force identification problem in least square sense, and assume for simplicity that $\overline{\mathbf{H}}$ has no zeros singular values. And then the Moore–Penrose pseudo inverse of $\overline{\mathbf{H}}$ can be formulated as follows

$$\overline{\mathbf{H}}^{+} = (\overline{\mathbf{H}}^{\mathrm{T}}\overline{\mathbf{H}})^{-1}\overline{\mathbf{H}}^{\mathrm{T}} = (\mathbf{V}\Sigma^2\mathbf{V}^{\mathrm{T}})^{-1}\mathbf{V}\Sigma\mathbf{U}^{\mathrm{T}} = \mathbf{V}\Sigma^{-1}\mathbf{U}^{\mathrm{T}} = \sum_{i=1}^{n} u_i^{\mathrm{T}}\sigma_i^{-1}v_i \tag{16}$$

And then the ordinary least square solution of force identification problem Eq. (10) can be written as

$$\mathbf{f}_{LS} = \sum_{i=1}^{n} \frac{u_i^{\mathrm{T}}\mathbf{y}}{\sigma_i} v_i \tag{17}$$

This equation clearly illustrates the difficulties with the ordinary least squares solution to Eq. (10), when the coefficients $|u_i^{\mathrm{T}}\mathbf{y}|$ corresponding to smaller singular values σ_i do not decay as fast as the singular values, the ordinary least squares solution $\mathbf{f}_{LS}$ is dominated by the terms in the sum corresponding to the relative small singular values σ_i. As a consequence, the solution $\mathbf{f}_{LS}$ has many sign changes and appears completely random. Thus the primary difficult with the inverse problem of force identification Eq. (7) is that they are essentially underdetermined due to the cluster of small singular values of $\overline{\mathbf{H}}$. Furthermore, if the measured response vector $\mathbf{y}$ is contaminated by the white noise, the noise in responses will be infinitely enlarged and the obtained solution is meaningless [17].

3.2. The regularization solution to the force identification problem

In general, any attempt to solve Eq. (10) with (17) will produce worthless results unless $\mathbf{f}$ is restricted by some conditions. Hence it is necessary to incorporate further information about the identified force in order to stabilize the problem and to single out a useful and stable solution, which is the purpose of regularization.

One of the most successful and widely known regularization methods is Tikhonov regularization or the damped least squares method. Tikhonov regularization technique was originally proposed independently by Tikhonov [20,21] and Phillips [22]. The restrictions on identified force $\mathbf{f}$ are imposed by a priory bound on $\|\mathbf{L}_i\mathbf{f}\|_2$ modifying Eq. (10)–(18), The Tikhonov regularization solution recasts the ordinary least square solution as Eq. (18), and the damped least square solution can be written as Eq. (19).

$$\min\left\{\|\overline{\mathbf{H}}\mathbf{f}_{reg} - \mathbf{y}\|_2^2 + \lambda\|\mathbf{L}_i\mathbf{f}_{reg}\|_2^2\right\} \tag{18}$$

$$\mathbf{f}_{reg} = \left(\overline{\mathbf{H}}^{\mathrm{T}}\overline{\mathbf{H}} + \lambda\mathbf{L}_i\right)^{-1}\overline{\mathbf{H}}^{\mathrm{T}}\mathbf{y} \tag{19}$$

where $\|\bullet\|_2^2$ denotes the Euclidean norm of the matrices, λ is a positive regularization parameter that controls the balance between the restrictions on $\mathbf{f}$ and the residual norm $\|\overline{\mathbf{H}}\mathbf{f}-\mathbf{y}\|_2^2$. $\mathbf{L}_i$ is typically a discrete approximation to the ith-order derivative. In this work the zeroth-order regularization is adopted as Ref. [12] and $\mathbf{L}_i$ is selected as identity matrix, i.e. $\mathbf{L}_0=\mathbf{I}$.

The major difficulty in applying the Tikhonov regularization technique lies in the ways to find an optimal regularization parameter λ. A good regularization parameter should yield a fair balance between the perturbation error and the regularization error in the regularized solution. Several methods have been proposed to determine the optimum regularization parameters [23–27]. L-curve criterion is one of the most notable ones to determine the regularization parameter. Hansen [24] reported that the L-curve criterion is a robust method to compute the optimum regularization parameter, but it tends to produce a regularization parameter that brings slightly over smooth solution. In this paper, the generalized cross-validation (GCV) criterion [16] is used to choose the optimum regularization parameters, and Hansen [23] pointed out that the GCV method indeed also seek to balance the perturbation and regularization error, in turn, is related to the corner of the L-curve. The GCV criterion is based on the philosophy that if an arbitrary element y_i of the right-hand side $\mathbf{y}$ is left out, then the corresponding regularized solution should predict this observation well, and the choice of the regularization parameter should be independent of an orthogonal transformation of $\mathbf{y}$, cf. [28] for more detail. This leads to choosing the regularization parameter which minimizes the GCV function

$$\mathbf{G}=\frac{\|\overline{\mathbf{H}}\mathbf{f}_{reg}-\mathbf{y}\|_2^2}{\left(trace\left(\mathbf{I}_m-\overline{\mathbf{H}}\overline{\mathbf{H}}^{reg}\right)\right)^2} \tag{20}$$

where $\overline{\mathbf{H}}^{reg}=\left(\overline{\mathbf{H}}\overline{\mathbf{H}}^{\mathrm{T}}+\lambda\mathbf{I}\right)^{-1}\overline{\mathbf{H}}^{\mathrm{T}}$ is a matrix which produces the regularized solution $\mathbf{f}_{reg}$ when multiplied with $\mathbf{y}$, ie. $\mathbf{f}_{reg}=\mathbf{H}^{reg}\mathbf{y}$. The dominator in Eq. (20) can be computed in $O(n)$ operations with the bidiagonalization algorithm in Ref. [16]. The proper regularization parameter λ can be chosen by minimization the GCV function and then a stable solution $\mathbf{f}_{reg}$ can be sought from Eq. (19).

4. Numerical experiment

To illustrate the efficiency of the proposed force identification algorithm based on the PTIM-MP, with the aid of the regularization technique to reconstruct the dynamic input force, two numerical experiments are described in this section. In case 1, two forces exerted on a plane truss framework are reconstructed. This numerical experiment is designed for verifying the effectiveness of the PTIM-MP with relatively large sampling time steps, and the stability of regularization solution is also validated simultaneous. In case 2, two forces acting on a free–free frame structure are identified. This case is mainly to illustrate the effectiveness of the proposed method with different measurement noise level, when the force identification model is ill-posed, notwithstanding the force identification model founded by PTIM-MP.

Normalized error measurements are used to access the force identification result. The root mean square (RMS) error in an estimated force $\mathbf{f}_{reg}$ is defined as

$$\varepsilon_{\%RMS}=\left(\frac{\sqrt{\sum(f(i)_{reg}-f(i)_{true})^2}}{\sqrt{\sum f(i)_{true}^2}}\right)100\% \quad (i=0,1,2,\ldots,N_t) \tag{21}$$

where $\mathbf{f}_{true}$ and $\mathbf{f}_{reg}$ are the actual force and the estimated one, respectively. In the force identification process, white noise is added, as Eq. (22), to the calculated responses in order to simulate practical engineering measurement.

$$\mathbf{y}_{noise}=\mathbf{y}_{cal}+NP\left(\frac{\sqrt{\sum y_i^2}}{N_t}\right)\eta \tag{22}$$

where $\mathbf{y}_{cal}$ is the N_t length column vector of calculated responses, $\mathbf{y}_{noise}$ is the noise corrupted version of $\mathbf{y}$ in Eq. (7) and η is the N_t length vector of normally distributed random numbers with zero mean and variance equal to 1. In general, NP is the measurement noise level ranging from 0.0 to 1.0.

4.1. Numerical test case 1: a plane truss framework

This plane truss framework consists of 21 link bars as shown in Fig. 1. The length of each horizontal and vertical pole is 5 m and the lumped mass 1×10^3 Kg is concentrated on every node. In this case study, the tensile stiffness is $3\times10^7\,\mathrm{Nm}^{-2}$ and the damping ratio of each mode is 0.02. The circular frequencies of this plane truss framework are obtained as Table 1. Two excitation forces taken as formula (18) are imposed on nodes 7 and 11 in the negative

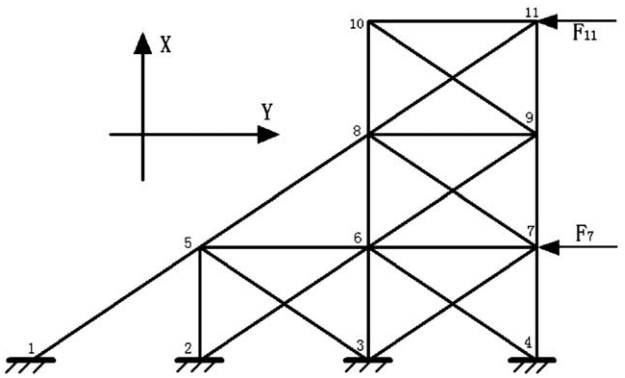

Fig. 1. The plane truss framework.

Table 1
The circular frequency of plane truss framework (Hz).

Mode	1	2	3	4	5	6	7
Frequency	16.92	40.75	46.41	78.88	94.67	99.37	106.19
Mode	8	9	10	11	12	13	14
Frequency	111.01	118.04	123.56	138.39	148.24	160.53	169.67

Table 2
Identification errors with different measurement noise and sampling time.

Plane truss framework					
Sampling time (s)			0.01	0.02	0.05
Identification error (%)	F7	1%	1.52	1.87	7.21
	F11	1%	6.88	6.98	11.34

direction of y axis.

$$\begin{cases} F_7 = 10(1-\cos(\pi t))\sin(3\pi t) \\ F_{11} = 100te^{-5t} \end{cases} \tag{23}$$

In this case, the acting time is two seconds and the sampling time interval Δt is 0.01 s, 0.02 s, 0.05 s, respectively. The 1 and 5 percent white noise is added to the calculated responses on nodes 6, 8 and 10, respectively, i.e. $NP = 0.01, 0.05$ in formula (22), and these corrupted responses are used to simulate the measured responses to reconstruct the time history of two input forces.

From the analysis in Section 3, the condition number of matrix $\overline{\mathbf{H}}$ in force identification model is increasing for a period of time as the time step is decreasing, i.e. N_t is increasing. The force identification problem will be ill-posed. However, the large sampling time is used, the round error of force identification model in numerical computation will affect the force identification results. The PTIM-MP can alleviate this difficulty caused by round error in computation. Table 2 shows the force identification error computed by formula (21), with different measurement sampling times and 1 percent white noise. We can see that the identification precision is decreasing as the sampling time argumentation. But the identification force time history obtained by PTIM-MP with the aid of regularization technique still agrees well with the input force in the whole time history, as Figs. 2 and 3 plots. Furthermore, the effectiveness of regularization technique is also validated, Figs. 4 and 5 illustrate the time history of the identified force on nodes 7 and 11 with sampling time 0.01 s and 1 percent measurement noise. The identified forces obtained by regularization technique and without regularization technique all agree well with the actual input forces, due to in this case used 1 percent white noise, the problem Eq. (11) can be considered as a well-posed problem. A condition that insures the stability and well-posedness of Eq. (11) is the Picard condition [29]. The Picard condition is satisfied when the coefficients $|u_i^{\mathrm{T}}\mathbf{y}|$ decay to zero more quickly than the singular values σ_i in the Picard plot. The Picard plot in Fig. 6 is shown that the Picard condition is met in case 1 used 1 percent white noise, and thus the results obtained without regularization technique is also reasonable. The Picard plot in Fig. 7, however, shows that the coefficients $|u_i^{\mathrm{T}}\mathbf{y}|$ decay to zeros more slowly than the singular values σ_i in case 1 used 5 percent white noise, hence the force identification problem is ill-posed, and the regularization is needed. The plots in Figs. 8 and 9, show

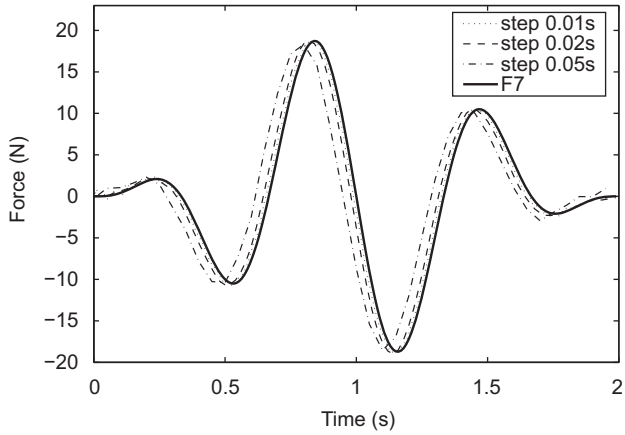

Fig. 2. Identification results on node 7 with 1 percent white noise and different sampling time.

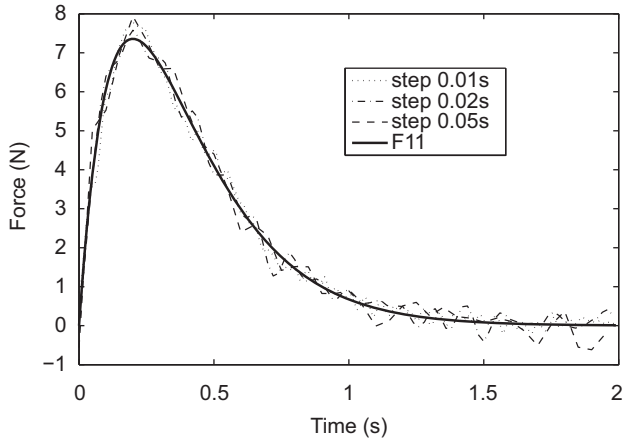

Fig. 3. Identification results on node 11 with 1 percent white noise and different sampling time.

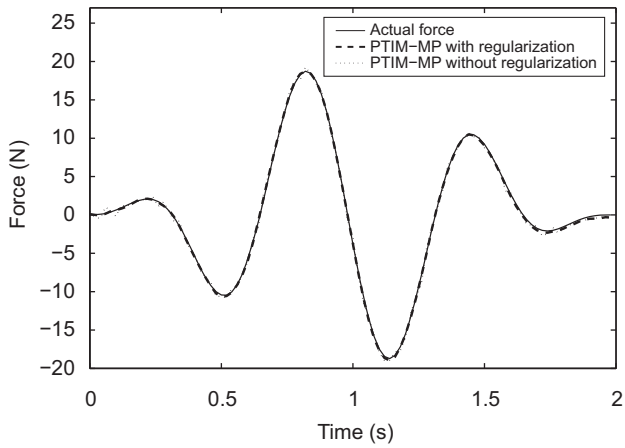

Fig. 4. Force identification results on node 7 with 1 percent white noise.

that the identification results obtained by the regularization are still identical with the actual inputs on the whole. It should be noted that the identification results obtained without regularization are meaningless and are not displayed in this article. Subsequently, another ill-posed force identification problem will be devised to demonstrate the effectiveness of PTIM-MP with the aid of regularization technique in the next test case.

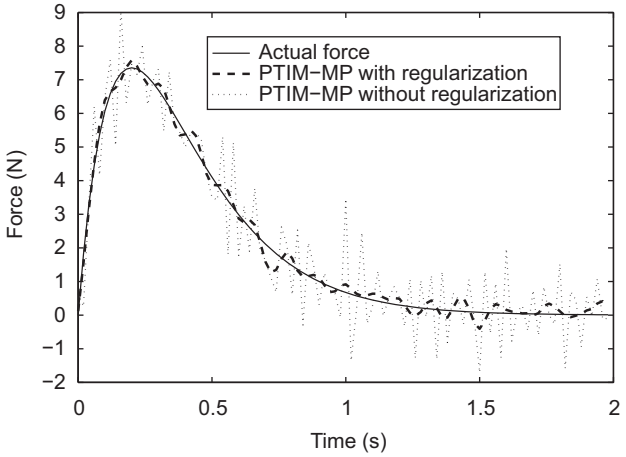

Fig. 5. Force identification results on node 11 with 1 percent white noise.

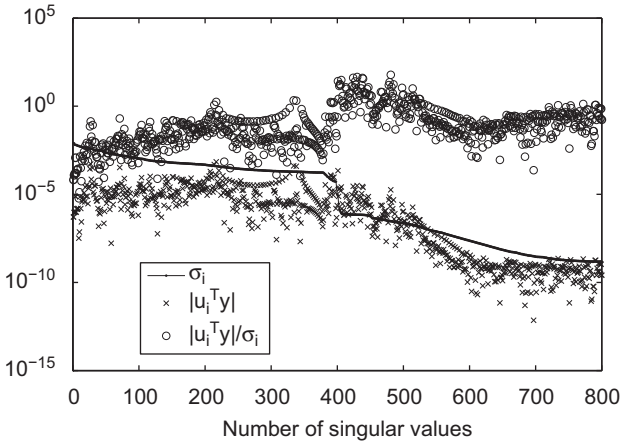

Fig. 6. The Picard plot for case 1 with 1 percent white noise in responses.

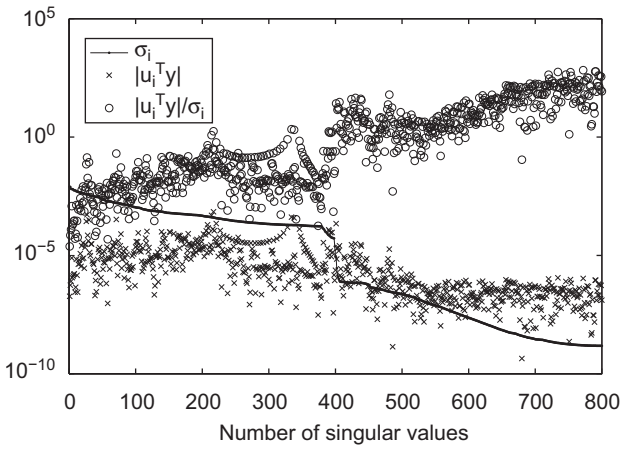

Fig. 7. The Picard plot for case 1 with 5 percent white noise in response.

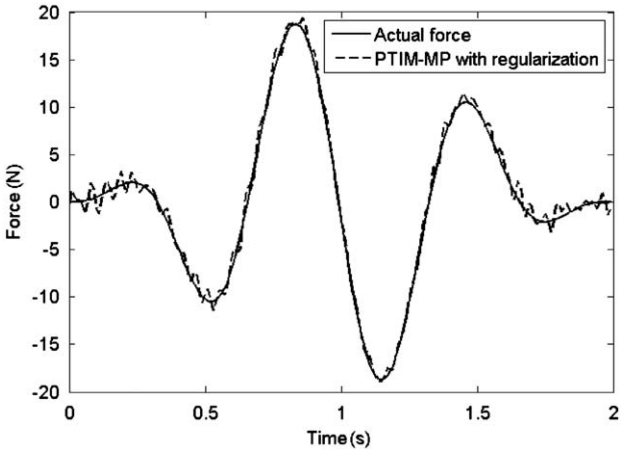

Fig. 8. Force identification results with 5 percent white noise in response.

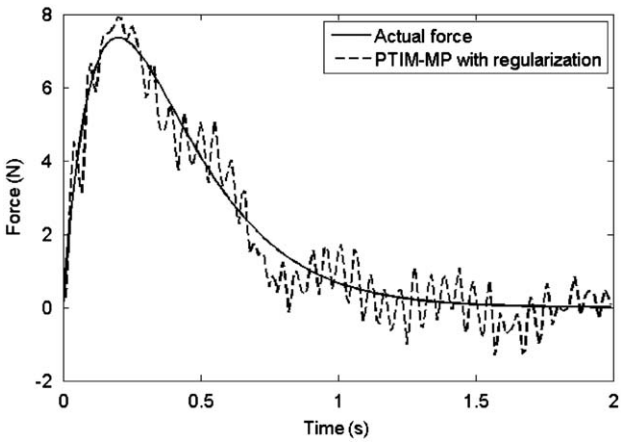

Fig. 9. Force identification results with 5 percent white noise in response.

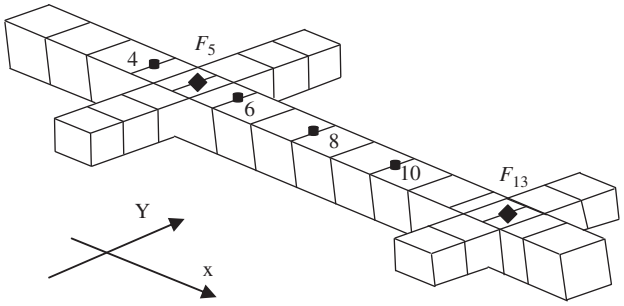

Fig. 10. The free–free frame structure.

4.2. Numerical test case 2: a free–free frame structure

A free–free frame structure is plotted in Fig. 10, consists of 24 beam elements, and each element has 6 degree of freedoms, the length and section is 0.5 m and 0.3 m × 0.3 m, respectively. The elastic modulus and the density are 300 MPa and 7800 kgm^{-3}, respectively. Two forces as formula (24) impact on nodes 5 and 13 in the direction of x axis as shown in Fig. 10.

$$\begin{cases} F_5 = 50(1-\cos(2\pi\omega t))\sin(6\pi\omega t) \\ F_{13} = 500t\exp(-4t)), \omega = 0.5 \end{cases} \tag{24}$$

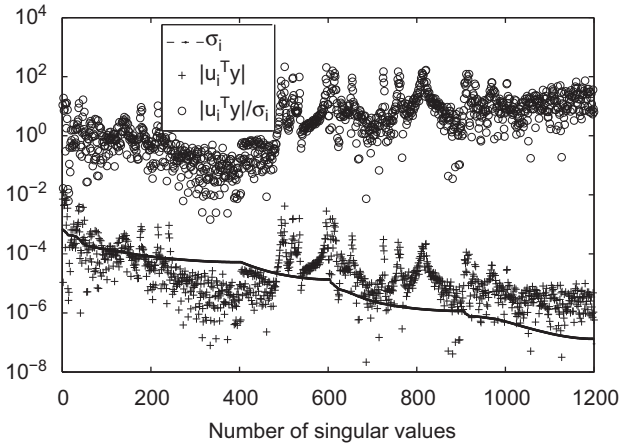

Fig. 11. The Picard plot for case 2.

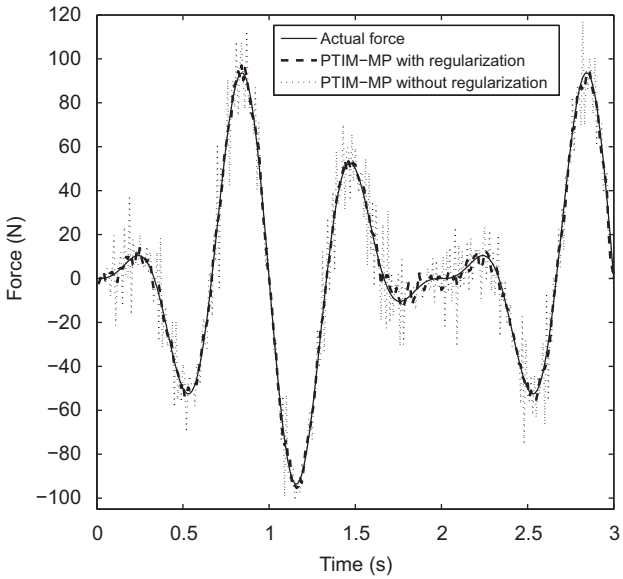

Fig. 12. Force identification results on node 5.

The responses on nodes 4, 6, 8 and 10 are measured for 3 s with sampling time 0.01 s. The white noise level *NP* in formula (21) equals 0.05.

In this case the force identification model is also founded by PTIM-MP. The Picard plot in Fig. 11 shows that the singular values σ_i, coefficients $|u_i^T\mathbf{y}|$ and the ratio $|u_i^T\mathbf{y}|/\sigma_i$ for increasing i, when the measurement responses y are polluted by 5 percent white noise. In this figure, the singular values σ_i of structural matrix $\overline{\mathbf{H}}$ decay gradually to zero and the ratio between the largest and smallest nonzero singular values is 7.2831×10^3. Based on these observations in Picard plot, one is able to conclude that this problem is ill-posed. Clearly, in Fig. 11, it is observed that the coefficients $|u_i^T\mathbf{y}|$ decrease more slowly than the singular values σ_i. The ratio $|u_i^T\mathbf{y}|/\sigma_i$ is increasing and the white noise in the measured responses $\mathbf{y}$ will be widely amplified and propagated into the reconstructed forces.

To overcome this issue of noise amplification in the inversion process, a regularization technique described in Section 3 is utilized and the optimum regularization parameterλ is selected as 9.1829×10^{-8} through the GCV criterion for the Tikhonov regularization in the standard form. Using this optimum parameter, one is able to obtain the reconstructed force F_5 and F_{13} as plotted in Figs. 12 and 13, respectively. Clearly, in these plots the white noise amplification in the inverse process is significantly reduced. The reconstructed forces obtained by the PTIM-MP with the aid of regularization technique match the actual inputs quite well and the RMS error of these reconstructed forces is 6.1 and 23.1 percent, respectively. While the identification results, achieved by PTIM-MP without regularization technique, have large

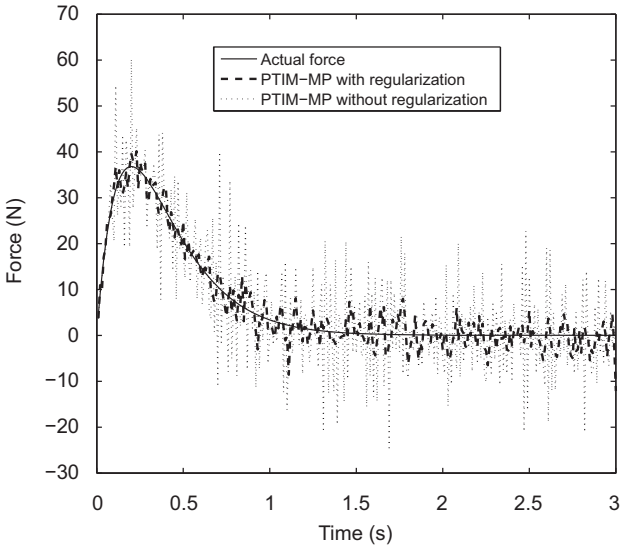

Fig. 13. Force identification results on node 13.

fluctuations, and the corresponding RMS error is 29.6 and 381.75 percent, respectively. However, the identification results with regularization technique are still a little fluctuation comparing with the actual inputs. This is mainly due to the fact that the white noise is intermingled with the dynamic information and purely mathematical techniques cannot absolutely dealt with this issue.

5. Conclusion

In general, the force identification problem mainly focuses on the affection of white noise in measured responses on the force identification results. In this work, we explore the influence of round error of force identification model on the identified results. PTIM-MP can precisely found the force identification model within the scope of general computer accuracy, while it does not cost much computing time. This precise force identification model can improve the force identification results in certain extent. However, it does not radically deal with the ill-posedness in force identification process, and the improved accuracy of force identification model may be still demolished by the white noise in measured response, thus the regularization technique is needed. Two numerical tests, especially the second, verify this point. Furthermore, it should be noted that, except for the white noise in measured responses and the round errors of force identification model, the sensor placement also affects the force identification results. From the results of two numerical tests, we can see that identification result of F_5 is better than that of F_{13} in numerical test case 2. This is mainly due to the measurement sensors placement on nodes 4, 6, 8 and 10, where the measurement responses mainly reflect the dynamic information ofF_5. Case 1 is in the same way, the obtained result of F_7 appears better than that of F_{11}, because the measurement response on nodes 6, 8 and 10 contains much more information of F_7 than that of F_{11}. The influence of sensor configuration on force identification is beyond the scope of this paper, and such issue will be discussed in future work. For a detailed discussion about the sensor placement for force identification, one can consult Refs. [30–31].

Acknowledgment

We are very thankful to reviewers for their valuable advice.

Appendix A. The derivation with exponential superposition method

In general, the second order differential equation of structural system is as follows

$$\mathbf{M}\ddot{\mathbf{x}}(t)+\mathbf{C}\dot{\mathbf{x}}(t)+\mathbf{K}\mathbf{x}(t)=\mathbf{r}(t) \tag{A.1}$$

where $\mathbf{M}$ denotes the symmetric and positive definite mass matrix, $\mathbf{C}$ and $\mathbf{K}$ denotes positive semidefinite damping and stiffness matrices, respectively. $\ddot{\mathbf{x}}(t)$, $\dot{\mathbf{x}}(t)$ and $\mathbf{x}(t)$ denotes the acceleration vector, velocity vector and displacement vector, respectively. The Eq. (A.1) can be written as Eq. (1) in Hamiltonian forms in state space, with the equation $\dot{\mathbf{x}}(t)=\dot{\mathbf{x}}(t)$ and

the transformation of Eqs. (A.2) and (A.3).

$$\mathbf{v}=\begin{bmatrix}\mathbf{x}^{\mathrm{T}} & \mathbf{p}^{\mathrm{T}}\end{bmatrix}^{\mathrm{T}},\quad \mathbf{H}=\begin{bmatrix}\mathbf{A} & \mathbf{D}\\ \mathbf{B} & \mathbf{E}\end{bmatrix},\quad \mathbf{f}=\begin{bmatrix}0^{\mathrm{T}} & \mathbf{r}^{\mathrm{T}}\end{bmatrix}^{\mathrm{T}} \tag{A.2}$$

$$\mathbf{p}=\mathbf{M}\dot{\mathbf{x}}+\tfrac{1}{2}\mathbf{C}\mathbf{x},\quad \mathbf{A}=-\tfrac{1}{2}\mathbf{M}^{-1}\mathbf{C}$$

$$\mathbf{B}=\tfrac{1}{4}\mathbf{C}\mathbf{M}^{-1}\mathbf{C}-\mathbf{K},\quad \mathbf{E}=-\tfrac{1}{2}\mathbf{C}\mathbf{M}^{-1},\quad \mathbf{D}=\mathbf{M}^{-1} \tag{A.3}$$

The quantity $\mathrm{e}^{-\mathbf{H}t}$ is multiplied on both sides of Eq. (1) in Section 2, and integrating the Eq. (A.4) in time interval $[t_0,t]$,

$$\mathrm{e}^{-\mathbf{H}t}\dot{\mathbf{v}}(t)=\mathrm{e}^{-\mathbf{H}t}\mathbf{H}\mathbf{v}(t)+\mathrm{e}^{-\mathbf{H}t}\mathbf{f}(t) \tag{A.4}$$

$$\begin{cases}\int_{t_0}^{t}\mathrm{e}^{-\mathbf{H}\tau}(\dot{\mathbf{v}}(\tau)-\mathbf{H}\mathbf{v}(\tau))\mathrm{d}\tau=\int_{t_0}^{t}\mathrm{e}^{-\mathbf{H}\tau}\mathbf{f}(\tau)\mathrm{d}\tau\\ \int_{t_0}^{t}\mathrm{d}\mathrm{e}^{-\mathbf{H}\tau}\mathbf{v}(\tau)=\int_{t_0}^{t}\mathrm{e}^{-\mathbf{H}\tau}\mathbf{f}(\tau)\mathrm{d}\tau\end{cases} \tag{A.5}$$

$$\mathbf{v}(t)=\mathbf{v}(t_0)\exp(\mathbf{H}(t-t_0))+\int_{t_0}^{t}\exp(\mathbf{H}(t-\tau))\mathbf{f}(\tau)\mathrm{d}\tau \tag{A.6}$$

Supposed the input force in integration time interval is constant, the Eq. (A.6) can be formulated as Eq. (2) in Section 2.

References

[1] K.K. Stevens, Force identification problems: an overview, *Proceeding of the SEM Spring Conference on Experimental Mechanics*, Houston, 1987, pp. 838–844.
[2] H. Innoue, J.J. Harrigan, S.R. Reid, Review of inverse analysis for indirect measurement of impact force, *Applied Mechanics Reviews* 54 (6) (2001) 503–525.
[3] B.J. Dobson, E. Rider, A review of the indirect calculations of excitation forces from measured structural response data, *Proceeding of the Institution of Mechanical Engineering Science* 204 (1990) 69–75.
[4] L.J.L. Nordstron, T.P. Nordberg, A critical comparison of time domain load identification methods, *Proceeding of the Sixth International Conference on Motion and Vibration Control* 2 (2002) 1151–1156.
[5] F.E. Gunawan, H. Homma, Y. Kanto, Two-step B-splines regularization method for solving an ill-posed problem of impact-force reconstruction, *Journal of Sound and Vibration* 297 (1–2) (2006) 200–214.
[6] L. Yu, T.H.T. Chan, Recent research on identification of moving loads on bridges, *Journal of Sound and Vibration* 305 (1–2) (2007) 3–21.
[7] L.J.L. Nordstrom, H. Johansson, F. Larsson, A strategy for input estimation with sensitivity analysis, *International Journal for Numerical Method in Engineering* 69 (11) (2007) 2219–2246.
[8] X.Q. Jiang, H.Y. Hu, Reconstruction of distributed dynamic loads on an Euler beam via mode-selection and consistent spatial expression, *Journal of Sound and Vibration* 316 (1–5) (2008) 122–136.
[9] M.S. Allen, T.G. Carne, Delayed, multi-step inverse structural filter for robust force identification, *Mechanical Systems and Signal Processing* 22 (5) (2008) 1036–1054.
[10] J.-J. Liu, C.-K. Ma, I.-C. Kung, D.-C. Lin, Input force estimation of a cantilever plate by using a system identification technique, *Computer Methods in Applied Mechanics and Engineering* 190 (11–12) (2000) 1309–1322.
[11] A.D. Stelzner, D.C. Kammer, P. Milenkovic, A time domain method for estimating forces applied to an unrestrained structure, *Journal of Vibration and Acoustics* 123 (4) (2001) 524–532.
[12] T. Patrik Nordberg, I. Gustafsson, Dynamic regularization of input estimation problems by explicit block inversion, *Computer Methods in Applied Mechanics and Engineering* 195 (44–47) (2006) 5877–5890.
[13] W. Zhong, *Symplectic Solution Methodology in Applied Mechanics*, Higher Education Press, Beijing, 2006 (in Chinese).
[14] E. Jacquelin, A. Bennani, P. Hamelin, Force reconstruction: analysis and regularization of a deconvolution problem, *Journal of Sound and Vibration* 265 (1) (2003) 81–107.
[15] Y. Liu, W. Steve Shepard Jr., Dynamic force identification based on enhanced least squares and total least-squares schemes in the frequency domain, *Journal of Sound and Vibration* 282 (1–2) (2005) 37–60.
[16] L. Elden, A note on the computation of the generalized cross-validation function for ill-conditioned least squares problems, *BIT* 24 (1984) 467–472.
[17] P.C. Hansen, Rank-deficient and discrete ill-posed problems: Numerical Aspects of Linear Inversion, *SIAM Philadelphia*, PA, 1998.
[18] P.C. Hansen, Deconvolution and regularization with Toeplitz matrices, *Numerical Algorithms* 29 (4) (2008) 323–378.
[19] G.H. Golub, C.F. Van Loan, *Matrix Computations*, (3rd Edition), John Hopkins University Press, 1996.
[20] A.N. Tikhonov, Solution of incorrectly formulated problems and the regularization method, *Soviet Mathematics Doklady* (4) (1963) 1035–1038.
[21] A.N. Tikhonov, Y. Arsenin, *Solution of Ill-posed Problems*, Wiley, New York, 1977.
[22] D.L. Phillips, A technique for the numerical solution of certain equations of the first kind, *Journal of the Association for Computing Machinery* 9 (1962) 84–97.
[23] P.C. Hansen, Analysis of discrete ill-posed problems by means of the L-curve, *SIAM Review* 34 (1992) 561–580.
[24] P.C. Hansen, D.P. O'Leary, The use of the L-curve in the regularization of discrete ill-posed problem, *SIAM Journal on Scientific Computing* 14 (1993) 1487–1503.
[25] R.D. Fierro, J.R. Bunch, Collinearity and total least squares, *SIAM Journal on Matrix Analysis and Applications* 15 (1994) 1167–1181.
[26] P.C. Hansen, Regularization, GSVD and truncated GSVD, *BIT* 29 (1989) 491–504.
[27] V.A. Morozov, *Methods for Solving Incorrectly Posed Problems*, Springer-Verlag, New York, 1984.
[28] G. Wahba, *Spline Models for Observational Data*, SIAM, Philadelphia, 1990.
[29] P.C. Hansen, Truncated SVD solutions to discrete ill-posed problems with ill-determined numerical rank, *SIAM Journal on Scientific Computing* 11 (1990) 503–518.
[30] X.L. Guo, D.S. Li, Experiment study of structural random loading identification by the inverse pseudo excitation method, *Journal of Structural Engineering and Mechanics* 18 (6) (2004) 791–806.
[31] D.S. Li, H.N. Li, C.P. Fritzen, A note on fast computation of effective independence through QR downdating for sensor placement, *Mechanical Systems and Signal Processing* 23 (2009) 1160–1168.